



Published in final edited form as:

Clin Cancer Res. 2010 May 1; 16(9): 2591–2604. doi:10.1158/1078-0432.CCR-09-2443.

TRAIL and doxorubicin combination induces pro-apoptotic and anti-angiogenic effects in soft tissue sarcoma *in vivo*

Suizhao Wang^{1,2}, Wenhong Ren^{1,2}, Jeffery Liu^{1,2}, Guy Lahat^{1,2}, Keila Torres^{1,2}, Gonzalo Lopez^{2,3}, Alexander J Lazar^{2,4}, Andrea Hayes-Jordan^{1,5}, Kebin Liu⁶, Jim Bankson⁷, John D. Hazle⁷, and Dina Lev^{2,3}

¹ Department of Surgical Oncology, University of Texas MD Anderson Cancer Center, Houston, TX

² The Sarcoma Research Center at the University of Texas MD Anderson Cancer Center, Houston, TX

³ Department of Cancer Biology, University of Texas MD Anderson Cancer Center, Houston, TX

⁴ Department of Pathology, University of Texas MD Anderson Cancer Center, Houston, TX

⁵ Department of Pediatrics, University of Texas MD Anderson Cancer Center, Houston, TX

⁶ Department of Biochemistry and Molecular Biology, Medical College of Georgia, Augusta, GA

⁷ Department of Imaging Physics, University of Texas MD Anderson Cancer Center, Houston, TX

Abstract

Purpose—Novel therapeutic approaches for complex karyotype soft tissue sarcoma (STS) are crucially needed. Consequently, we assessed the efficacy of tumor necrosis factor-related apoptosis-inducing ligand (TRAIL), in combination with chemotherapy, on local and metastatic growth of human STS xenografts *in vivo*.

Experimental Design—TRAIL was evaluated alone and combined with low dose doxorubicin in two human STS SCID mouse xenograft models utilizing fibrosarcoma (HT1080; wild-type *p53*) and leiomyosarcoma (SKLMS1; mutated-*p53*), testing for impact on local growth, metastasis, and overall survival. MRI was used to evaluate local growth and bioluminescence was used to longitudinally assess lung metastases. Tissues were evaluated via immunohistochemistry and TUNEL staining for treatment effects on tumor cell proliferation, apoptosis, angiogenesis, angiogenic factors, and TRAIL receptor expression. qRT-PCR angiogenesis array was utilized to assess therapy-induced gene expression changes.

Results—TRAIL/doxorubicin combination induced marked STS local and metastatic growth inhibition in a *p53* independent manner. Significantly increased ($p < 0.001$) host survival I was also demonstrable. Combined therapy induced significant apoptosis, decreased tumor cell proliferation, and increased TRAIL receptor (DR4 and DR5) expression in all treated tumors. Moreover, decreased microvessel density was observed, possibly secondary to increased expression of the anti-angiogenic factor CXCL10 and decreased pro-angiogenic IL-8 cytokine in response to TRAIL/doxorubicin combination, as was also observed *in vitro*.

Address for reprint request: Corresponding author - Dina Lev, MD, Department of Cancer Biology, MD Anderson Cancer Center, 1515 Holcombe Blvd, Unit 1104, Houston TX 77030, Phone: 713-792-1637, Fax: 713-563-1185, dlev@mdanderson.org.

Conflicts of interest: None

*Part of the data included in the current manuscript was presented at the 100th AACR annual meeting (4/2009, Denver, CO) as a Minisymposium oral presentation (#2055)

Conclusions—Given the urgent need for better systemic approaches to STS, clinical trials evaluating TRAIL in combination with low dose chemotherapy are potentially warranted.

Keywords

Soft tissue sarcoma; TRAIL; doxorubicin; apoptosis; angiogenesis; Therapy

Introduction

Complex karyotype soft tissue sarcoma (STS; e.g., leiomyosarcoma and unclassified pleomorphic sarcoma) pose a significant therapeutic challenge (1). Surgical resection combined with radiotherapy is the optimal approach for localized STS management (2). However, STS exhibit a marked propensity for local and systemic failure, frequently manifesting therapeutic resistance. Doxorubicin, the single most active anti-STS chemotherapeutic agent, has a disappointing 30% overall responderate. After initial chemoresponsiveness, breakthrough tumor progression and local and/or distant recurrence are frequently observed (3,4), contributing to a 50% five year STS overall survival rate that has remained stagnant for nearly 50 years. Accordingly, more effective therapeutic approaches to complex karyotype STS are critically needed.

One of the hallmarks of STS and other malignancies is their pronounced resistance to apoptosis, resulting in cell survival even when confronted by multiple stress stimuli. Tumor necrosis factor-related apoptosis inducing ligand (TRAIL/Apo2L), a member of the TNF superfamily, activates the extrinsic pathway of apoptosis via interaction with death receptors (5). Five receptors are known to bind TRAIL, two of which (DR4 and DR5) initiate an apoptotic cascade upon TRAIL binding. Interestingly, TRAIL has been shown to selectively induce apoptosis in a variety of transformed and cancer cell lines *in vitro* and *in vivo* without adversely affecting normal cells (6–8). While other death receptor ligands such as TNF α and FasL cause septic shock and hepatotoxicity *in vivo*, TRAIL is tolerated well in mice and non-human primates (9). These novel TRAIL properties have resulted in the consideration of recombinant TRAIL and agonistic anti-TRAIL receptor antibodies in clinical trials for human cancer (10).

Preclinical studies evaluating TRAIL effects in sarcoma are limited and focus mainly on simple karyotype fusion gene STS (i.e., Rhabdomyosarcoma, Ewing Sarcoma, and osteosarcoma; 11–13). Varying responses have been recorded; in general, sarcoma cell lines and freshly prepared primary cultures were relatively TRAIL resistant (14,15). The mechanism of TRAIL resistance is not well understood and may involve multiple TRAIL-induced apoptotic pathway components. For example, alteration of TRAIL receptors via genetic and epigenetic changes can lead to enhanced TRAIL resistance (12,16,17). Similarly, expression of molecules that can interfere with caspase-8 activation, such as FLIP, may confer TRAIL resistance (18–20). Moreover, overexpression of anti-apoptotic molecules such as BCL2 and survivin or decreased expression/function of pro-apoptotic mediators (e.g., BAX) have also been implicated (21).

While the exact mechanisms remain under investigation, the observed resistance of human cancers to TRAIL *in vivo* has prompted searches for combination therapies with superior efficacy. Several chemotherapeutic and biological agents have been evaluated for their capacity to sensitize tumor cells to TRAIL-mediated apoptosis (22–24). Recent investigations suggest that combining TRAIL with clinically relevant anti-STS chemotherapies (e.g., doxorubicin) might overcome TRAIL resistance, resulting in significantly augmented apoptotic cell death *in vitro* (16,17,24). However, the effect of this therapeutic approach on STS local and metastatic growth *in vivo* has not been determined. The goal of studies presented here was to bridge this knowledge gap by evaluating the effect of combined TRAIL/doxorubicin on the growth of human fibrosarcoma and leiomyosarcoma xenografts in immunocompromised mice. Results

demonstrate that combined therapy significantly inhibits local and metastatic STS growth while no major effect was elicited by either of the compounds administered alone. Anti-STS effects were due to enhanced tumor cell apoptosis and disrupted tumor associated angiogenesis. Taken together, our study strongly supports combining TRAIL and chemotherapy as a novel therapeutic approach for complex karyotype STS.

Materials and Methods

Cells lines and reagents

Human soft tissue sarcoma cell lines HT1080 (fibrosarcoma; wild type p53) and SKLMS1 (leiomyosarcoma; mutated p53) were obtained from ATCC. Authentication of cell lines was conducted immediately prior to their use for the current studies utilizing Short Tandem Repeat (STR) DNA fingerprinting conducted at the MDACC Cell Line Core facility. HT1080 cells were transduced to stably express luciferase (HT.GL). These cells were cultured in DMEM supplemented with 10% FCS (Life Technologies, Inc). Doxorubicin (Ben Venue Lab, Bedford, OH) was obtained from the UTMDACC pharmacy. Recombinant human TRAIL was produced as previously described (9). In brief, cDNA of the extracellular domain of TRAIL corresponding to amino acids 114–281 was subcloned into the pET17/b (Novagen) bacterial expression vector and expressed in the BL21(DE3)pLysE (Novagen) bacterial host. Following induction of TRAIL expression using isopropyl- β -thio-galactosidase (IPTG; 1 mM), bacterial pellets were harvested, and TRAIL was purified following passage through a nickel column (Ni-NTA) followed by a size exclusion column (Amersham). TRAIL activity was confirmed by treating TC71 cells (TRAIL sensitive Ewing sarcoma cells) with the compound and evaluating apoptosis rate by PI staining/FACS analysis as described below.

Commercially available antibodies were used for immunohistochemical detection of PCNA (DAKO, Glostrup, Denmark), DR4 (Active Motif, Carlsbad, CA), DR5 (IMGENEX, San Diego, CA), Ki67 (Thermo Scientific, Fremont, CA), CD31 (BD Bioscience, San Diego, CA), IL8 (Invitrogen, Carlsbad, CA), CXCL10 (R & D System, Minneapolis, MN), VEGF (R&D Systems, Minneapolis, MN), neutrophils (anti-neutrophil Ab NIMP-R14; Abcam, Cambridge, MA) and macrophages (F4-80; Serotec, Oxford, UK). Dead End Fluorometric TUNEL System (Promega, Madison, WI) was used for TUNEL staining. Secondary antibodies included HRP-conjugated (Universal kit HRP; Biocare Medical, Concord, CA) and fluorescent secondary antibodies (anti-rabbit Alexa488, anti-mouse Alexa 594); Jackson Immuno Research, West Grove, PA). Other reagents included CytoQ FC Receptor block (Innovex Bioscience, Richmond, CA), Hoechst 33342 (Polysciences, Inc., Warrington, PA) and propyl gallate (ACROS Organics, Morris Plains, NJ).

Cell growth assay

MTS assays were conducted using CellTiter96 Aqueous Non-Radioactive Cell Proliferation Assay kit (Promega, Madison, WI), per manufacturer's instructions. Absorbance was measured at a wavelength of 490 nm, and the absorbance values of treated cells are presented as a percentage of the absorbance of untreated cells.

Apoptosis assays

Cell cycle analysis was conducted to determine the sub-G1 fraction. In brief, STS cell monolayers were treated with relevant agents for time periods as indicated. Fixed cells were treated with 50 μ g/ml RNase and stained with 50 μ g/ml propidium iodide for 30 min. Cells were analyzed in a FACSCalibur, and data were analyzed with Cell Quest and Flowjo software (Philadelphia, PA) or ModFitLT v3.1 software (Verity Software House). A caspase-3 apoptosis assay was also utilized. DEVD-NucViewTM 488 caspase-3 assay kit for live cells (cat #30029)

was purchased from Biotium, INC (Hayward, CA). Apoptotic cells were detected per manufacturer's instructions.

qRT-PCR

Five µg total RNA was used for cDNA synthesis by RT III kit (Invitrogen, Carlsbad, CA) according to manufacturers' instructions. Real time quantitative PCR was performed using PCR Master Mix (Promega, Madison, WI) and relevant primers (sequences are available per request). Gene expression was analyzed using a Mastercycler Eppendorf realplex (Eppendorf, Hamburg Germany). The levels of gene expression were normalized using GAPDH levels based on the comparative threshold cycle method.

ELISA

CXCL10 and IL8 levels were measured in STS cell conditioned media after indicated treatments using enzyme-linked immunosorbent assay (ELISA). The assay was constructed and performed following manufacturer's instructions (R&D, Minneapolis, MN).

In vivo therapeutic experiments

All animal procedures and care were approved by the MD Anderson Cancer Center Institutional Animal Care and Usage Committee. Animals received humane care as per the Animal Welfare Act and the NIH "Guide for the Care and Use of Laboratory Animals." Animal models were utilized as previously described (26,27). Trypan blue staining confirmed viable STS cells (SKLMS1 and HT1080 $1 \times 10^6/0.1$ mL HBSS/mouse) were injected subcutaneously into the flank of six week old female SCID mice ($n = 40$ /experiment), growth was measured twice weekly; after establishment of palpable lesions mice (~5mm in average size; 12d after HT1080 injection and 16d after SKLMS1 injection) were assigned to four treatment groups (10/group): (a) control (vehicles only); (b) doxorubicin (1.2 mg/kg biweekly i.p.; low-dose schedule, based on our previous experience results in minimal side effects; (26,27); (c) TRAIL (10 mg/kg, 5-day per week i.p.; based on previous studies using TRAIL for other tumor types (9,28), this dose is lower than the MTD in mice (150–200 mg/kg) and was selected to minimize side effects when combined with chemotherapy); and, (d) doxorubicin plus TRAIL. Treatment with doxorubicin was initiated on day one while TRAIL was given starting day two of treatment. Mice were followed for tumor size (by tumor measurement and MRI described below), well being, and body weight and sacrificed when control group tumors reached an average of 1.5 cm in their largest dimension. Tumors were resected, weighed, and frozen or fixed in formalin and paraffin-embedded for IHC studies.

An experimental lung metastasis STS model was used to evaluate metastases growth and survival. HT1080 stably transduced to express GFP-luciferase cells (HT1080GL; $1 \times 10^6/0.1$ mL HBSS/mouse) were injected into the tail vein of female SCID mice. Lung metastases development and growth were evaluated utilizing bioluminescent imaging (BLI) technology as previously described (27). When BLI suggested established lung metastases (14 days after injection), mice were assigned to treatment groups as per above. Mice were followed for BLI readout and body weight, and sacrificed when control group tumors exhibited high luciferase readout. During necropsy, lungs were excised, visible metastases counted, and the lungs were fixed in formalin and paraffin embedded for IHC studies. Similarly, in a second set of experiments mice were evaluated for survival.

MRI

Animals were anesthetized with 5% isoflurane in oxygen and maintained using 0.5%–2% isoflurane in oxygen. A linear volume resonator with 35 mm inner diameter (ID) was used for signal excitation and detection. At baseline, animals were scanned using a 4.7T Biospec small

animal MRI system (Bruker Biospin MRI, Billerica, MA). T1-weighted FLASH (TE = 3.5ms, TR = 11ms, 30° excitation) and 3-plane RARE (TE = 48ms, TR = 2000ms, ETL = 8) acquisitions were used to confirm animal placement. A T2-weighted coronal RARE sequence (TE = 65ms, TR = 3000ms, ETL = 12, FOV = 4cm × 3cm on a 256 × 192 image matrix, 2 averages, 1mm slice thickness with 0.25mm skip) was used to localize tumor, and axial T1-weighted spin-echo (TE = 8.4ms, TR = 900ms) and T2-weighted RARE images (TE = 80ms, TR = 3000ms, ETL = 12, 5 averages) with matching slice prescriptions (FOV = 3cm × 2.5cm on a 256 × 192 image matrix, 0.75mm slice thickness) were used for tumor visualization. Scheduling conflicts at end of treatment necessitated MRI scanning using a 7T Biospec System (Bruker Biospin MRI, Billerica, MA). T1-weighted FLASH and 3-plane RARE acquisitions were again used during animal placement, and a T2-weighted coronal RARE sequence (TE = 65ms, TR = 5000ms, ETL = 12, FOV = 4cm × 3cm on a 256 × 192 image matrix, 0.75mm slice thickness with 0.25mm skip) was for tumor localization. Axial T1-weighted spin-echo (TE = 11.5ms, TR = 900ms, 2 averages) and T2-weighted RARE images (TE = 57ms, TR = 3500ms, ETL = 12, four averages) with matching slice prescriptions (FOV = 4cm × 3cm on a 256 × 192 image matrix, 0.75mm slice thickness with 0.25mm skip) were used for tumor visualization.

Immunohistochemistry and TUNEL assays

Immunohistochemical assays and TUNEL staining were performed as previously described (26,27). To detect invading neutrophils and macrophages frozen section slides were examined: 1:1000 and 1:600 primary antibody dilutions were used, respectively. Staining distribution and intensity was evaluated and scored by at least two (including SW, WR, and KT) independent reviewers blinded to the therapeutic group to which each slide belonged. PCNA scoring was determined as the average of percent positive immunoreactive cells evaluated by counting tumor cells in five high power fields (X400). For TUNEL scoring average number of positive nuclei was calculated in five high power microscopic fields (X400) selected from a central region in viable tumor areas avoiding areas containing necrosis. Five of the most vascularized areas within a tumor (“hot spots”) identified based on CD31 positivity were chosen at low magnification and vessels were counted in a representative high-magnification (X400) field in each of these areas. Blood vessel density was calculated as the summation of all counts divided by five. Number of invading neutrophils and macrophages were quantitated by counting positively staining cells in five high power fields (X400).

Angiogenesis RT² Profiler PCR Array

Total RNA was isolated from frozen xenograft tumor specimens of control and doxorubicin/TRAIL combination treated mice using Trizol Reagent (Invitrogen, Carlsbad, CA). After DNase treatment, RNA was further cleaned up using Qiagen RNeasy[®] Mini Kit (Qiagen, Valencia, CA). cDNA was synthesized by RT² First Strand kit (SABiosciences, Frederick, MD) following the company’s instructions. Gene expression profiling using the Angiogenesis RT² Profiler PCR Array (SABiosciences, Frederick, MD) was conducted. This platform is designed to profile the expression of 84 key genes in angiogenesis (for a comprehensive list of genes included in this array see www.sabiosciences.com). qRT-PCR was conducted using Mastercycler Eppendorf realplex (Eppendorf AG, Hamburg, Germany) based on array manufacturers’ instructions. Relative gene expression was determined using the $\Delta\Delta CT$ method. Data was further analyzed by PCR Array Data Analysis Web Portal (www.SABiosciences.com/pcrarraydataanalysis.php).

Statistical analysis

Cell culture based assays were repeated at least three times and mean \pm SD was calculated. Cell lines were examined separately. For qRT-PCR arrays experiments were repeated twice for

both STS models using different tumor samples. For outcomes that were measured at a single time point, two-sample *t*-tests were used to assess the differences. Differences in xenograft growth (tumor/metastases) *in vivo* were assessed using a two-tailed Student's *t*-test. Kaplan-Meier curves were constructed to determine overall survival time. Significance was set at $P \leq 0.05$. All statistical analyses were carried out using SPSS software.

Results

TRAIL/doxorubicin combination induces STS cell apoptosis *in vitro*

Two cell lines were selected for investigation: human leiomyosarcoma (SKLMS1) and fibrosarcoma (HT1080); both reproducibly grow as tumors in immunocompromised mice histologically recapitulating counterpart human lesions. SKLMS1 harbors a mutated *p53* (a common mutation in complex karyotype STS) and HT1080 harbors a *NRAS* mutation but is *p53* wild type (www.sanger.ac.uk/genetics/CGP/cosmic). We first investigated the effect of low dose doxorubicin/TRAIL combination on *in vitro* cell growth. The effect of TRAIL alone (25ng/ml/24hr), doxorubicin alone (0.1 μ M/48hr), or their combination (doxorubicin for 24hr followed by the addition of TRAIL for another 24hr) on cell growth was evaluated using MTS assays. Only minimal growth inhibition was observed in either cell line after treatment with TRAIL or doxorubicin alone at doses and time-points as indicated above (Fig 1A). In contrast, the combination of both agents resulted in a significant growth reduction ($p < 0.005$). These findings were further strengthened by the significant increase ($p < 0.05$) in sub-G1 cell population and enhanced caspase-3 activity observed after treatment with combination therapy (Fig 1B&C). Taken together, these results indicate that combining doxorubicin and TRAIL results in superior growth inhibition and apoptosis in STS cells as compared to either compound alone and that this effect is independent of *p53* mutation status, further supporting the *in vivo* evaluation of this novel therapeutic regimen. Interestingly, the superior effect of combined therapy was not observed when drugs were delivered together or when TRAIL was administered prior to doxorubicin (data not shown), possibly suggesting that doxorubicin sensitizes STS cells to TRAIL and providing a rationale for *in vivo* studies scheduling.

TRAIL/doxorubicin combination inhibits the growth of human leiomyosarcoma *in vivo*

First, we investigated the effect of TRAIL and doxorubicin on human leiomyosarcoma growth in SCID mice. Treatments were highly tolerated; no significant weight loss was observed. Treatment with low-dose doxorubicin alone resulted in a small, non-statistically significant decrease in tumor growth; the average tumor volume of doxorubicin treated tumors at study termination was $1453 \text{ mm}^3 \pm 481$ compared $1738 \text{ mm}^3 \pm 533$ for controls ($p = 0.33$, Fig 2A). Similarly, TRAIL alone resulted in only a slight decrease in tumor growth compared to controls ($1535 \text{ mm}^3 \pm 742$; $p = 0.57$). In contrast, combined low-dose doxorubicin and TRAIL was markedly inhibitory (tumor volume: $685 \text{ mm}^3 \pm 216$) compared to control, doxorubicin alone, or TRAIL alone ($p < 0.01$). Mouse monitoring ($n = 3/\text{group}$) using magnetic resonance imaging (MRI; Bruker Biospin MRI, Billerica, MA) further confirmed the above results (Fig 2B). A scan conducted on the therapy start date demonstrated similar average tumor volumes in all four mouse cohorts. In contrast, a significant difference in tumor volume was identified at the end of the study; tumors of the combination group were significantly smaller ($456 \text{ mm}^3 \pm 144$; $p < 0.05$) than those in control, doxorubicin alone, or TRAIL alone groups ($1692 \text{ mm}^3 \pm 204$, $1374 \text{ mm}^3 \pm 330$, and $1292 \text{ mm}^3 \pm 318$, respectively).

Tumor sections containing viable cells from each treatment group were selected to evaluate the impact of the different therapies on STS cell proliferation and apoptosis (Fig 2C). Scoring of IHC staining for PCNA (a nuclear marker for proliferation) demonstrated a statistically significant reduction in proliferation of leiomyosarcoma cells in the combination treated vs. control, doxorubicin, or TRAIL treated groups ($80\% \pm 11$ vs. $69\% \pm 2$, $73\% \pm 15$, $27\% \pm 13$,

respectively; $p < 0.05$). Similarly, TUNEL assay staining (marker for apoptosis) analysis revealed that combined doxorubicin and TRAIL induced a statistically significant increase in leiomyosarcoma apoptosis (control: 9 ± 5 ; doxorubicin: 13 ± 7 ; TRAIL: 18 ± 9 ; and combination: 99 ± 23 TUNEL positive cells, respectively; $p < 0.001$). Previous studies suggested that a possible mechanism responsible for the synergistic effect of TRAIL combined with chemotherapy *in vitro* might be secondary to induction of TRAIL receptor(s) expression (12,29); to evaluate if this process occurs in leiomyosarcoma *in vivo*, IHC for DR4 and DR5 was performed (Fig 2D). Control treated tumors expressed only minimal levels of DR4 while a demonstrable increase in its expression was noticed in all treated specimens: a higher level was seen in doxorubicin-treated samples than in TRAIL-treated samples, and was most pronounced in combination therapy group. Similarly only low DR5 expression was seen in control tumors. However, in contrast to DR4 expression only a minimal increase in DR5 expression was noticed in TRAIL treated tumors and a moderate increase was seen after doxorubicin treatment alone whereas combination therapy resulted in a marked increase in expression intensity and distribution of this TRAIL receptor. It is possible that increased TRAIL receptor expression, especially DR5, is at least partially responsible for the enhanced anti-tumorigenic effect of combined TRAIL/doxorubicin.

TRAIL/doxorubicin combination inhibits the local and metastatic growth of human fibrosarcoma *in vivo* and prolongs survival

Next, we evaluated the effect of combined TRAIL/doxorubicin on another human STS histological subtype; HT1080 xenografts growing in SCID mice. As depicted in Fig 3A, treatment with doxorubicin or TRAIL alone did not significantly affect HT1080 growth compared to control-treated mice ($p = 0.73$ and 0.65 , respectively). However, combined treatment resulted in significant tumor growth inhibition compared to the other three experimental arms ($p < 0.01$). Moreover, average tumor weights at termination of the study were similar in control, doxorubicin, and TRAIL alone treated mice ($1.27 \text{g} \pm 0.54$, $1.19 \text{g} \pm 0.45$, $1.119 \text{g} \pm 0.43$, respectively) whereas combination therapy significantly reduced tumor weight ($0.30 \text{g} \pm 0.29$) compared to all other therapeutic regimens ($p < 0.001$).

Similar to above, Ki-67 staining and TUNEL assay scoring revealed that combined doxorubicin/TRAIL combination resulted in significantly decreased tumor cell proliferation ($p < 0.05$) and increased apoptosis ($p < 0.05$; control group: $65\% \pm 13$ and 3 ± 2 ; doxorubicin group: $47\% \pm 15$ and 5 ± 4 ; TRAIL group: $50\% \pm 12$ and 11 ± 5 ; and combination group: $14\% \pm 7$ and 72 ± 15 , respectively; Fig 3B). The baseline DR4 and DR5 expression levels in control HT1080 tumors were higher than those of SKLMS1 tumors (Fig 3B). An increase in DR4 expression was observed in all treatment cohorts most pronounced in doxorubicin and TRAIL/doxorubicin treatment groups. Similarly, an increase in DR5 was seen in doxorubicin treated tumors and to the highest extent in combination treated samples. This pattern of TRAIL receptors expression was similar in both of the STS histological subtype animal models evaluated.

Metastases (especially pulmonary) are the main cause of STS-specific mortality (30). To evaluate whether combining doxorubicin/TRAIL resulted in pulmonary metastatic outgrowth inhibition, we utilized an experimental fibrosarcoma lung metastasis model. No major difference in luciferase readout was observed between doxorubicin or TRAIL alone treated mice compared to controls (Fig 4A). In contrast, combined TRAIL/doxorubicin resulted in decreased luciferase readout with fewer and smaller lung metastases observed on the lung surface. Macroscopic findings were also confirmed on H+E staining, demonstrating large lung tumor deposits in control, doxorubicin, and TRAIL groups and smaller, microscopic lesions in the combination group. Lung weights were significantly lower in combined vs. control, doxorubicin or TRAIL treatment groups ($0.38 \text{g} \pm 0.12$ vs. $0.97 \text{g} \pm 0.14$, $0.91 \text{g} \pm 0.13$, and $0.83 \text{g} \pm 0.10$, respectively; $p < 0.005$, Fig 4B)

Lastly, we evaluated the effect of combined TRAIL/doxorubicin on the survival of mice harboring lung metastases. An experiment as per above was conducted and mice (n=6–7/group) were followed for survival. The median survival time of control, doxorubicin, and TRAIL treated mice was 20, 21, and 20 days, respectively, compared to 34d for mice treated with TRAIL and doxorubicin. A KM plot is shown in Fig 4C, demonstrating a statistically significant prolongation in overall survival of mice treated with combined TRAIL/doxorubicin (p=0.001).

TRAIL/doxorubicin combination elicits anti-angiogenic effects in STS

STS are highly vascular and angiogenic, perhaps accounting for their capacity to grow to large size and avidly metastasize (31). Therefore, we evaluated if the combined therapeutic approach affected STS microvessel density (MVD; Fig 5A). Treatment with doxorubicin or TRAIL alone resulted in a statistically non-significant reduction in the number of CD31 positive vessels compared to controls (SKLMS1: 85±23 and 90±27 vs. 110±32, respectively; HT1080: 71±21 and 63±14 vs. 80±39, respectively). In contrast, combination therapy resulted in a marked reduction in CD-31 positive vessels (21±11 and 32±15 in SKLMS1 and HT1080, respectively; p<0.05). Interestingly, no TUNEL staining was identified in CD-31 positive cells upon Immunofluorescence double staining in any one of the treatment cohorts (Fig 5A). These results suggest that the observed decrease in blood vessel number in response to combined therapy is not secondary to endothelial cell apoptosis and possibly represents *de novo* inhibition of angiogenesis.

Tumor-associated angiogenesis is a complex process involving many pro- and anti- angiogenic factors. Next, we sought to evaluate the effect of TRAIL/doxorubicin combination on the expression of angiogenic factors *in vivo*. RNA extracted from control and combination treated tumors was subjected to an angiogenesis RT² Profiler RT PCR array. This array only recognizes human RNA; therefore, results represent gene expression changes in STS cells and not in the murine-originating tumor-associated stroma. Interestingly, expression changes in only two genes of those included on the array (n=84) were found to occur reproducibly in both STS models; a marked increase in the level of the anti-angiogenic factor CXCL10 (7.4 ± 5.5 fold and 9.9 ± 3.0 fold in SKLMS1 and HT1080, respectively) and a significant decrease in the expression of the angiogenic factor IL-8 (9.5 ± 2.3 fold and 8.2 ± 2.5 fold in SKLMS1 and HT1080, respectively) was observed in the TRAIL/doxorubicin treated tumors compared to control treated tumors (p<0.05; Fig 5B). qRTPCR was used to evaluate mRNA expression of CXCL10 and IL-8 in an independent tumor sample cohort of control, TRAIL, doxorubicin and combined TRAIL/doxorubicin SKLMS1 and HT1080 treated xenografts (Fig 5C). A significant increase (p<0.005) in CXCL10 mRNA expression was observed in combination treated tumors as compared to controls; no significant change was noted in TRAIL or doxorubicin alone treated tumors. Similarly, a statistically significant (p<0.005) decrease in IL-8 mRNA expression was observed in combination therapy tumors, but not in tumors treated with either compound alone. Treatment-induced effects on CXCL10 and IL-8 protein were further confirmed via IHC (Fig 5D). The functional impact of decreased IL8, one of the most important chemotactic factors for neutrophils, was further reflected by a statistically significant decrease in the number of tumor infiltrating neutrophils identified in combination treated samples (p<0.05; Figure 5D). Similarly, an increase in macrophage infiltration was observed in TRAIL/doxorubicin treated specimens possibly reflecting the enhanced activity of CXCL10 in these tumors and the recruitment of myeloid derived cells with anti-tumorigenic capacities (M1 macrophages; p<0.05, Figure 5D). Previously published data suggested a TRAIL-induced reduction in VEGF-A expression as a potential mechanism for TRAIL anti-angiogenic effects in glioblastoma (32). No effect of TRAIL/doxorubicin on VEGF-A level in STS specimens was demonstrated in the gene expression arrays, qRTPCR, and IHC (data not shown).

Lastly, we evaluated whether the *in vivo* effect of doxorubicin/TRAIL on CXCL10 and IL-8 expression could be recapitulated in culture. SKLMS1 and HT1080 cells were treated with doxorubicin (0.1 μ M), TRAIL (25ng/ml), or their combination with doxorubicin administered prior to TRAIL as described; RNA was extracted and conditioned media collected. As shown in Fig 6A, combined therapy resulted in a significant increase in CXCL10 mRNA expression and a reduction in IL-8 mRNA expression compared to controls or either drug alone ($p < 0.05$). Similarly, ELISA confirmed the respective changes in protein expression levels of these cytokines (Fig 6B). While the studies above do not preclude possible effects of TRAIL/doxorubicin on other angiogenesis-related factors, a possible role for CXCL10 induction and IL8 decrease in the anti-angiogenic effects resulting from this therapeutic regimen is suggested in STS.

Discussion

A potential role for TRAIL as a novel anti-cancer agent has emerged due to its potent and possibly tumor selective pro-apoptotic effects. Several Phase I clinical trials evaluated the effects of TRAIL agonist monoclonal antibodies in patients with advanced solid cancers, including sarcoma (33,34). While no objective responses were recorded (as might be anticipated in Phase I trials), prolonged disease stabilization was documented in several sarcoma patients. For example, Plummer *et al* recently reported a study utilizing lexatimumab in which 12 sarcoma patients participated (34). Their results identified three sarcoma patients (extraosseous osteosarcoma, retroperitoneal liposarcoma, and chondrosarcoma), all with documented progressive disease on standard chemotherapy, in whom lexatimumab resulted in prolonged disease stabilization and minimal sideeffects. Together, these clinical studies suggest that TRAIL agonist effects are not specific sarcoma histological subtype selective. However, their apparent limited clinical impact when used as single anti-sarcoma agents calls for the identification of more effective combinatorial therapeutic approaches.

Studies here demonstrate that the combination of doxorubicin (the most commonly utilized anti-STS chemotherapeutic agent) and TRAIL, administered in this sequential order, elicits potent local and metastatic growth inhibitory effects in xenograft models of human STS, whereas no significant effect was observed with either agent alone. These data further expand previously published findings suggesting that chemotherapy might enhance TRAIL-mediated apoptosis in sarcoma cells *in vitro* (25,35–37). Importantly, our findings show that the doxorubicin/TRAIL combination effect is independent of *p53* mutation status: significant anti-tumor effects were observed in STS harboring either wild type or mutated *p53*. This observation is of potential clinical relevance in STS because *p53* dysregulation is very common, and STS harboring *p53* mutations are thought to be more resistant to current therapeutic strategies (38).

The molecular mechanisms resulting in combined doxorubicin and TRAIL pro-apoptotic synergistic effects are not well defined. While the sensitivity of cells to TRAIL does not appear to be a simple function of TRAIL death receptor expression level, the augmentation of TRAIL-induced apoptosis by chemotherapeutic drugs has been suggested to be at least partly the result of drug-induced up-regulation of death receptors (14,25,36). Concordantly, our studies demonstrated increased DR4 and DR5 expression in STS specimens treated with combined doxorubicin/TRAIL. Chemotherapy effects on TRAIL downstream signaling and modulation of pro- and anti-apoptotic effector expression has also been suggested (28). For example, chemotherapy-induced decrease in cFLIP expression was identified as a potential mechanism of osteosarcoma cell sensitization to TRAIL (9,36). Alternatively, decreased X-IAP expression was also observed (39). Further exploration of pertinent contributory mechanisms will facilitate combined doxorubicin and TRAIL therapy evaluation in human clinical trials.

In addition to the pro-apoptotic effects induced by the doxorubicin/TRAIL combination, studies here identified a significant reduction in the number of STS-associated blood vessels in response to therapy, albeit without evidence of endothelial cell apoptosis. STS are markedly angiogenic and highly dependent on their vasculature for local growth and metastasis (31). Thus, anti-angiogenic therapies affecting STS-associated vasculature hold major promise and several are under evaluation in human STS clinical trials (40–42). Interestingly, although TRAIL is commonly thought to have no or minimal effects on normal cells, recent studies have found unanticipated TRAIL pro-angiogenic enhanced endothelial cell proliferation, migration and cytoskeletal reorganization *in vitro* and *in vivo* to an extent comparable to VEGF (43,44). In contrast, other reports suggest a direct pro-apoptotic effect of TRAIL on endothelial cells (45). Moreover, decreased VEGF secretion, migration, and microvessel formation was shown after TRAIL treatment of HUVECs (32). The discrepancy between these studies might be a result of the different TRAIL concentrations utilized; while the former studies evaluated the effect of high TRAIL doses, the latter studies used markedly lower TRAIL concentrations (~10 fold). Studies presented here demonstrate that within the STS microenvironment treatment with TRAIL alone resulted in decreased MVD although to a statistically non-significant level, suggesting that at these concentrations TRAIL does not enhance angiogenesis but instead elicits an anti-angiogenic effect which is even more pronounced with combined TRAIL and doxorubicin. As in other solid tumors, STS-associated angiogenesis a complex process regulated by numerous pro- and anti-angiogenic factors.

The lack of TRAIL-induced endothelial cell apoptosis observed in STS xenografts raises the possibility that the anti-angiogenic effects are secondary to modulation of STS cell angiogenic factor expression. A previous report suggested that TRAIL inhibits angiogenesis in human glioblastoma via decreased tumor cell VEGF expression (32). No change in VEGF expression was observed in human STS xenografts after treatment with TRAIL alone or in combination with doxorubicin suggesting cancer- and even cell- type dependent TRAIL-induced effects. However, a significant increase in the expression of the anti-angiogenic cytokine CXCL10 (46) and a decrease in the levels of the pro-angiogenic cytokine IL8 (47) were observed in STS *in vivo* and *in vitro* after combination therapy but not with either compound alone. Furthermore, treatment induced changes in these cytokines can potentially affect tumor growth by impacting additional tumor microenvironment constituents such as neutrophils and macrophages in favor of tumor inhibition. The molecular mechanisms resulting in these treatment effects and the potential role of these cytokines in TRAIL/doxorubicin angiogenesis blockade are currently being investigated. Lastly, as these are secreted cytokines, evaluating their circulating blood levels as markers of treatment response is highly feasible; such analysis should be considered for inclusion in further preclinical studies and in human TRAIL/doxorubicin clinical trials. Taken together, our studies suggest that doxorubicin/TRAIL combination has significant anti-STS effects resulting in both tumor cell apoptosis and anti-angiogenic impact. Consequently, the merits of this therapeutic regimen should be potentially studied in STS clinical contexts.

Translational Relevance

The relative rarity and molecular diversity of complex karyotype soft tissue sarcoma (STS) has hampered progress in the management of this cohort of devastating malignancies. Novel therapeutic approaches are crucially needed. Studies here demonstrate that combining tumor necrosis factor-related apoptosis-inducing ligand (TRAIL) with chemotherapy yields marked anti-STS effects in human STS xenografts that model local and metastatic growth *in vivo*. These effects are *p53* mutation status independent and are a result of both direct tumor cell apoptosis and abrogation of STS-induced angiogenesis. These data offer new insights into the molecular effects of TRAIL/chemotherapy combinations and support further study of this approach in STS clinical contexts.

Acknowledgments

Financial Support: This manuscript was supported in part by an NIH/NCI RO1CA138345 grant (to DL) and by two separate Amschwand foundation seed grants (to SW and DL)

This research was kindly supported by an NIH/NCI RO1CA138345 grant (to DL) and by two separate Amschwand foundation seed grants (to SW and DL). We appreciate the expert assistance provided by Mr. Paul Cuevas in the preparation and submission of this manuscript, and Ms. Kim Vu is thanked for her aid in figure preparation.

References

1. Singer S, Demetri GD, Baldini EH, Fletcher CD. Management of soft-tissue sarcomas: an overview and update. *Lancet Oncol* 2000;1:75–85. [PubMed: 11905672]
2. Clark MA, Fisher C, Judson I, Thomas JM. Soft -tissue sarcomas in adults. *N Engl J Med* 2005;353:701–11. [PubMed: 16107623]
3. Bramwell VH, Anderson D, Charette ML. Doxorubicin-based chemotherapy for the palliative treatment of adult patients with locally advanced or metastatic soft tissue sarcoma. *Cochrane Database Syst Rev* 2003;CD003293. [PubMed: 12917960]
4. Cormier JN, Huang X, Xing Y, et al. Cohort analysis of patients with localized, high-risk, extremity soft tissue sarcoma treated at two cancer centers: chemotherapy-associated outcomes. *J Clin Oncol* 2004;22:4567–74. [PubMed: 15542808]
5. Hymowitz SG, Christinger HW, Fuh G, et al. Triggering cell death: the crystal structure of Apo2L/TRAIL in a complex with death receptor 5. *Molecular cell* 1999;4:563–71. [PubMed: 10549288]
6. Johnstone RW, Frew AJ, Smyth MJ. The TRAIL apoptotic pathway in cancer onset, progression and therapy. *Nat Rev Cancer* 2008;8:782–98. [PubMed: 18813321]
7. Srivastava RK. TRAIL/Apo-2L: mechanisms and clinical applications in cancer. *Neoplasia* 2001;3:535–46. [PubMed: 11774036]
8. Mitsiades CS, Treon SP, Mitsiades N, et al. TRAIL/Apo2L ligand selectively induces apoptosis and overcomes drug resistance in multiple myeloma: therapeutic applications. *Blood* 2001;98:795–804. [PubMed: 11468181]
9. Ashkenazi A, Pai RC, Fong S, et al. Safety and antitumor activity of recombinant soluble Apo2 ligand. *J clin invest* 1999;104:155–62. [PubMed: 10411544]
10. Fesik SW. Promoting apoptosis as a strategy for cancer drug discovery. *Nat Rev Cancer* 2005;5:876–85. [PubMed: 16239906]
11. Fulda S. Targeting apoptosis resistance in rhabdomyosarcoma. *Curr Cancer Drug Targets* 2008;8:536–44. [PubMed: 18781899]
12. Mitsiades N, Poulaki V, Mitsiades C, Tsokos M. Ewing's sarcoma family tumors are sensitive to tumor necrosis factor-related apoptosis-inducing ligand and express death receptor 4 and death receptor 5. *Cancer Res* 2001;61:2704–12. [PubMed: 11289151]
13. Van Valen F, Fulda S, Schafer KL, et al. Selective and nonselective toxicity of TRAIL/Apo2L combined with chemotherapy in human bone tumour cells vs. normal human cells. *Int J Cancer* 2003;107:929–40. [PubMed: 14601052]
14. Bouralexis S, Clayer M, Atkins GJ, et al. Sensitivity of fresh isolates of soft tissue sarcoma, osteosarcoma and giant cell tumour cells to Apo2L/TRAIL and doxorubicin. *Int J Oncol* 2004;24:1263–70. [PubMed: 15067350]
15. Tomek S, Koestler W, Horak P, et al. Trail-induced apoptosis and interaction with cytotoxic agents in soft tissue sarcoma cell lines. *Eur J Cancer* 2003;39:1318–29. [PubMed: 12763223]
16. Arizono Y, Yoshikawa H, Naganuma H, Hamada Y, Nakajima Y, Tasaka K. A mechanism of resistance to TRAIL/Apo2L-induced apoptosis of newly established glioma cell line and sensitisation to TRAIL by genotoxic agents. *Br J Cancer* 2003;88:298–306. [PubMed: 12610517]
17. Matsui TA, Sowa Y, Yoshida T, et al. Sulforaphane enhances TRAIL-induced apoptosis through the induction of DR5 expression in human osteosarcoma cells. *Carcinogenesis* 2006;27:1768–77. [PubMed: 16571651]
18. Thome M, Schneider P, Hofmann K, et al. Viral FLICE-inhibitory proteins (FLIPs) prevent apoptosis induced by death receptors. *Nature* 1997;386:517–21. [PubMed: 9087414]

19. Muhlethaler-Mottet A, Balmas K, Auderset K, Joseph JM, Gross N. Restoration of TRAIL-induced apoptosis in a caspase-8-deficient neuroblastoma cell line by stable re-expression of caspase-8. *Ann NY Acad Sci* 2003;1010:195–9. [PubMed: 15033719]
20. Yang D, Wang S, Brooks C, et al. IFN regulatory factor 8 sensitizes soft tissue sarcoma cells to death receptor-initiated apoptosis via repression of FLICE-like protein expression. *Cancer research* 2009;69:1080–8. [PubMed: 19155307]
21. Dan'ura T, Kawai A, Morimoto Y, Naito N, Yoshida A, Inoue H. Apoptosis and expression of its regulatory proteins in soft tissue sarcomas. *Cancer Lett* 2002;178:167–74. [PubMed: 11867201]
22. Wu XX, Kakehi Y. Enhancement of lexatumumab-induced apoptosis in human solid cancer cells by Cisplatin in caspase-dependent manner. *Clin Cancer Res* 2009;5:2039–47. [PubMed: 19276256]
23. Kim M, Liao J, Dowling ML, Voong KR, Parker SE, Wang S, El-Deiry WS, Kao GD. TRAIL inactivates the mitotic checkpoint and potentiates death induced by microtubule-targeting agents in human cancer cells. *Cancer Res* 2008;68:3440–9. [PubMed: 18451172]
24. Tsai WS, Yeow WS, Chua A, Reddy RM, Nguyen DM, Schrupp DS, Nguyen DM. Enhancement of Apo2L/TRAIL-mediated cytotoxicity in esophageal cancer cells by cisplatin. *Mol Cancer Ther* 5:2977–90. [PubMed: 17172403]
25. Komdeur R, Meijer C, Van Zweeden M, et al. Doxorubicin potentiates TRAIL cytotoxicity and apoptosis and can overcome TRAIL-resistance in rhabdomyosarcoma cells. *Int J Oncol* 2004;25:677–84. [PubMed: 15289869]
26. Lopez G, Liu J, Ren W, et al. Combining PCI-24781, a novel histone deacetylase inhibitor, with chemotherapy for the treatment of soft tissue sarcoma. *Clin Cancer Res* 2009;15:3472–83. [PubMed: 19417021]
27. Ren W, Korchin B, Lahat G, et al. Combined vascular endothelial growth factor receptor/epidermal growth factor receptor blockade with chemotherapy for treatment of local, uterine, and metastatic soft tissue sarcoma. *Clin Cancer Res* 2008;14:5466–75. [PubMed: 18765538]
28. Wu XX, Kakehi Y, Mizutani Y, et al. Doxorubicin enhances TRAIL-induced apoptosis in prostate cancer. *Int J Oncol* 2002;20:949–54. [PubMed: 11956588]
29. Shankar S, Chen X, Srivastava RK. Effects of sequential treatments with chemotherapeutic drugs followed by TRAIL on prostate cancer *in vitro* and *in vivo*. *The Prostate* 2005;62:165–86. [PubMed: 15389801]
30. Billingsley KG, Lewis JJ, Leung DH, Casper ES, Woodruff JM, Brennan MF. Multifactorial analysis of the survival of patients with distant metastasis arising from primary extremity sarcoma. *Cancer* 1999;85:389–95. [PubMed: 10023707]
31. Saenz NC, Heslin MJ, Adsay V, et al. Neovascularity and clinical outcome in high-grade extremity soft tissue sarcomas. *Ann Surg Oncol* 1998;5:48–53. [PubMed: 9524708]
32. Cantarella G, Risuglia N, Dell'eva R, et al. TRAIL inhibits angiogenesis stimulated by VEGF expression in human glioblastoma cells. *Br J Cancer* 2006;94:428–35.
33. Tolcher AW, Mita M, Meropol NJ, et al. Phase I pharmacokinetic and biologic correlative study of mapatumumab, a fully human monoclonal antibody with agonist activity to tumor necrosis factor-related apoptosis-inducing ligand receptor-1. *J Clin Oncol* 2007;25:1390–5. [PubMed: 17416859]
34. Plummer R, Attard G, Pacey S, et al. Phase 1 and pharmacokinetic study of lexatumumab in patients with advanced cancers. *Clin Cancer Res* 2007;13:6187–94. [PubMed: 17947486]
35. Hotta T, Suzuki H, Nagai S, et al. Chemotherapeutic agents sensitize sarcoma cell lines to tumor necrosis factor-related apoptosis-inducing ligand-induced caspase-8 activation, apoptosis and loss of mitochondrial membrane potential. *J Orthop Res* 2003;21:949–57. [PubMed: 12919886]
36. Evdokiou A, Bouralexis S, Atkins GJ, et al. Chemotherapeutic agents sensitize osteogenic sarcoma cells, but not normal human bone cells, to Apo2L/TRAIL-induced apoptosis. *Int J Cancer* 2002;99:491–504. [PubMed: 11992538]
37. Clayer M, Bouralexis S, Evdokiou A, Hay S, Atkins GJ, Findlay DM. Enhanced apoptosis of soft tissue sarcoma cells with chemotherapy: A potential new approach using TRAIL. *J Orthop Surg* 2001;9:19–22.
38. Zhan M, Yu D, Lang A, Li L, Pollock RE. Wild type p53 sensitizes soft tissue sarcoma cells to doxorubicin by down-regulating multidrug resistance-1 expression. *Cancer* 2001;92:1556–66. [PubMed: 11745235]

39. Mirandola P, Sponzilli I, Gobbi G, et al. Anticancer agents sensitize osteosarcoma cells to TNF-related apoptosis-inducing ligand downmodulating IAP family proteins. *Int J Oncol* 2006;28:127–33. [PubMed: 16327988]
40. Sleijfer S, Ray-Coquard I, Papai Z, et al. Pazopanib, a multikinase angiogenesis inhibitor, in patients with relapsed or refractory advanced soft tissue sarcoma: a phase II study from the European organisation for research and treatment of cancer-soft tissue and bone sarcoma group (EORTC study 62043). *J Clin Oncol* 2009;27:3126–32. [PubMed: 19451427]
41. Kuenen BC, Taberner J, Baselga J, et al. Efficacy and toxicity of the angiogenesis inhibitor SU5416 as a single agent in patients with advanced renal cell carcinoma, melanoma, and soft tissue sarcoma. *Clin Cancer Res* 2003;9:1648–55. [PubMed: 12738717]
42. Baker LH, Rowinsky EK, Mendelson D, et al. Randomized, phase II study of the thrombospondin-1-mimetic angiogenesis inhibitor ABT-510 in patients with advanced soft tissue sarcoma. *J Clin Oncol* 2008;26:5583–8. [PubMed: 18981463]
43. Secchiero P, Gonelli A, Carnevale E, et al. Evidence for a proangiogenic activity of TNF-related apoptosis-inducing ligand. *Neoplasia* 2004;6:364–73. [PubMed: 15256058]
44. Zauli G, Pandolfi A, Gonelli A, et al. Tumor necrosis factor-related apoptosis-inducing ligand (TRAIL) sequentially upregulates nitric oxide and prostanoid production in primary human endothelial cells. *Circ Research* 2003;92:732–40.
45. Gochuico BR, Zhang J, Ma BY, Marshak-Rothstein A, Fine A. TRAIL expression in vascular smooth muscle. *Am J Physiol Lung Cell Mol Physiol* 2000;278:1045–50.
46. Indraccolo S, Pfeffer U, Minuzzo S, et al. Identification of genes selectively regulated by IFNs in endothelial cells. *J Immunol* 2007;178:1122–35. [PubMed: 17202376]
47. Li A, Dubey S, Varney ML, Dave BJ, Singh RK. IL-8 directly enhanced endothelial cell survival, proliferation, and matrix metalloproteinases production and regulated angiogenesis. *J Immunol* 2003;170:3369–76. [PubMed: 12626597]

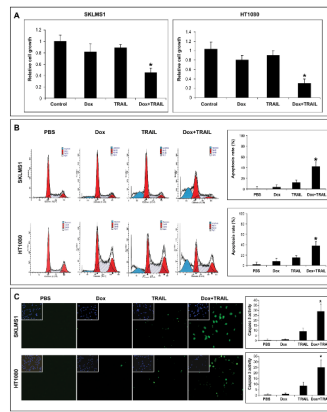


Figure 1.

Doxorubicin (Dox) and TRAIL combination results in superior pro-apoptotic effects in STS cells *in vitro*. A) The combination of doxorubicin (0.1 μ M/48hr) and TRAIL (25 μ g/ml/24hr) exhibits superior STS growth inhibition effects that either compound alone (MTS assays; * p <0.005); B) The combination of doxorubicin (0.1 μ M/48hr) and TRAIL (25 μ g/ml/24hr) elicits significant apoptosis in STS cells (PI/FACS analysis; * p <0.05); C) Pro-apoptotic effect is also demonstrated via caspase-3 activity assay (* p <0.05). Graphs represent the average of three repeated experiments \pm SD.

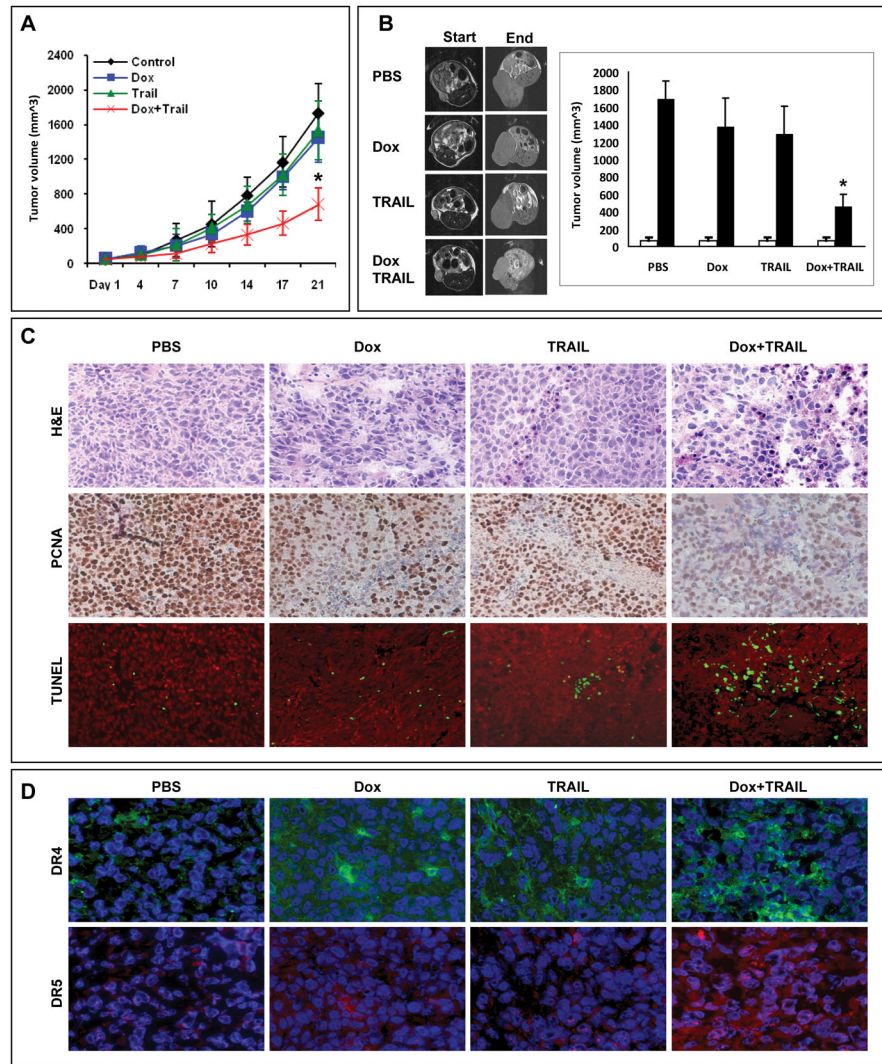


Figure 2. Doxorubicin (1.2mg/kg/biweekly) followed by TRAIL (10mg/kg, five days per week) decreases leiomyosarcoma (SKLMS1) growth *in vivo*. A) Tumor growth curves per treatment group (10mice/group); B) Representative MRI images of STS xenografts at time of treatment initiation and by the end of the study. Graphs depict average tumor volume as calculated from MRI images (n=3/group; *p<0.05). White bars represent tumor volume at treatment initiation and black bars at study termination; C) PCNA immunohistochemistry and TUNEL staining (red = nuclei, green =TUNEL) of SKLMS1 xenograft specimens (selected for presence of viable tumor shown in H+E); and, D) DR4 (green) and DR5 (red) immunofluorescent staining of SKLMS1 xenografts (nuclei are depicted in blue).

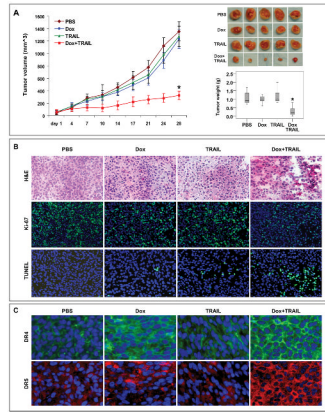


Figure 3. Doxorubicin and TRAIL combination decreases fibrosarcoma (HT1080) growth *in vivo*. A) Tumor growth curves per treatment group (left; n=10mice/group, p<0.01) and tumor pictures (right upper panel). Box plots (right lower panel) depict average tumor weights at termination of the study (p<0.001); B) Ki-67 immunofluorescence (blue =nuclei, green = Ki-67) and TUNEL staining (blue = nuclei, green =TUNEL) of HT1080 xenograft specimens (selected for presence of viable tumor shown in H+E); C) DR4 (green) and DR5 (red) immunofluorescent staining of HT1080 xenografts (nuclei are depicted in blue).

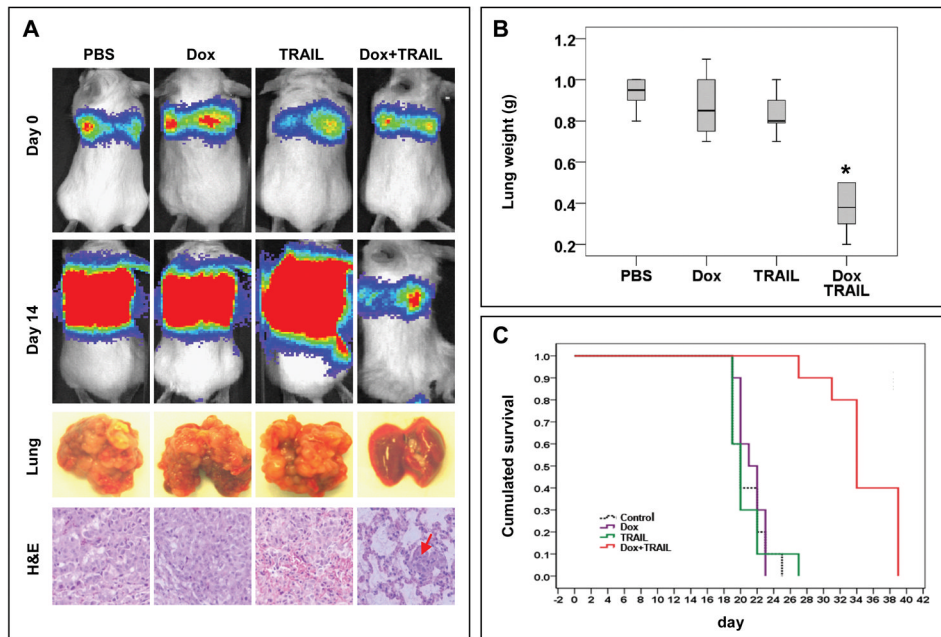


Fig 4. Doxorubicin and TRAIL combination inhibits fibrosarcoma (HT1080) lung metastases growth and enhances survival. A) BLI images of one representative mice of each treatment arm are shown demonstrating the markedly decreased luciferase readout in combination treated mice compared to control or either compound alone. Pictures and H+E staining demonstrate the reduction in lung metastatic deposits (arrows) in combination treated mice; B) Box plots demonstrating the significant decrease in lung weight of combination treated mice (* $p < 0.005$); C) Kaplan Meier survival curves demonstrating a statistically significant prolongation in overall survival of mice treated with doxorubicin/TRAIL combination ($p = 0.001$)

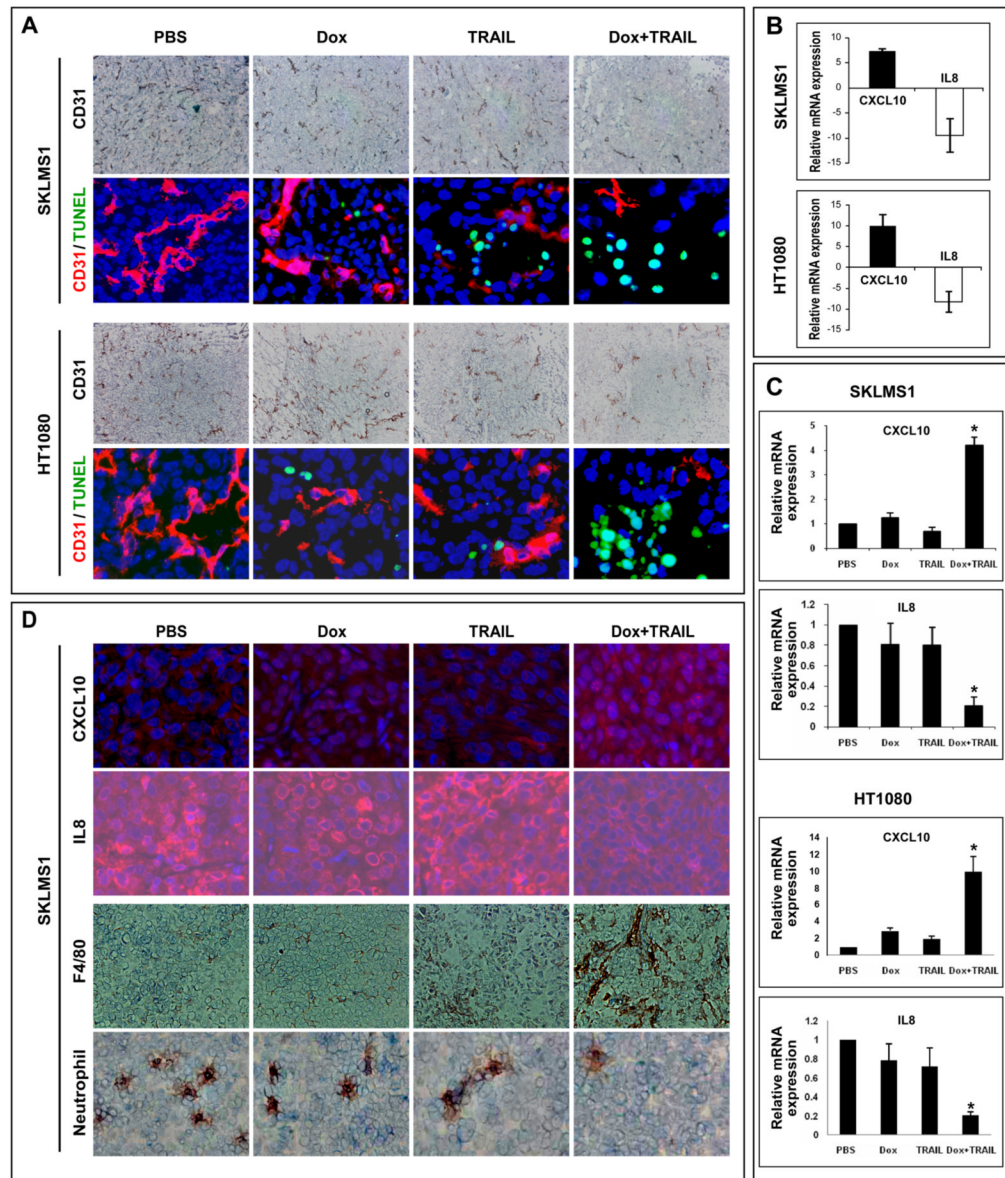


Fig 5. Doxorubicin and TRAIL combination inhibits STS associated angiogenesis. A) CD31 immunohistochemistry and CD31/TUNEL double immunofluorescence (CD31 = red, TUNEL = green) demonstrate decrease in blood vessel density in combination treatment samples but no evidence of endothelial cell apoptosis; B) Angiogenesis RT PCR array demonstrated a significant increase in CXCL10 mRNA expression and a marked decrease in IL8 mRNA levels in combination treated tumor samples of both STS xenograft models; C) Effects of treatment on CXCL10 and IL8 mRNA expression was further confirmed via RT PCR using an independent cohort of tumor samples (* $p < 0.05$). No significant gene expression changes were noticed in samples treated with either agent alone; D) effect of treatment on IL8 (red) and CXCL10 (red) protein expression *in vivo* was evaluated by immunofluorescence (nuclei = blue). An increase in tumor infiltrating macrophages and a decrease in tumor infiltrating neutrophils was also observed in TRAIL/doxorubicin treated tumors. Graphs represent the average of three repeated experiments \pm SD.

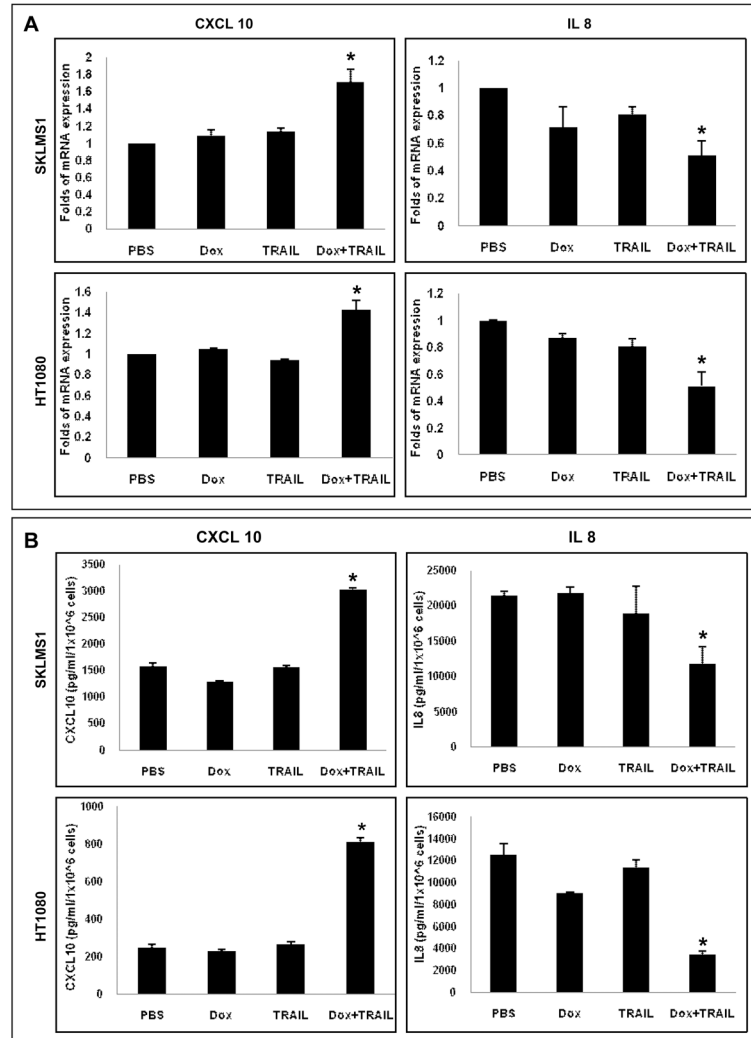


Fig 6. Doxorubicin and TRAIL combination modulates angiogenesis-related factor expression in STS cells. A) STS cells grown in culture were treated with doxorubicin (0.1 μ M/24hr), TRAIL (25 μ g/ml/12hr), or their combination. qRT-PCR demonstrated a significant increase in CXCL10 mRNA levels (* p <0.05) and a decrease in IL-8 mRNA expression (* p <0.05); B) Conditioned media was collected from STS cells treated as above and was subjected to ELISA. A significant increase in CXCL10 protein expression (* p <0.05) and a decrease in IL8 protein levels (* p <0.05) were observed. Graphs represent the average of three repeated experiments \pm SD.